Intergrowth Structures: The Chemistry of Solid–Solid Interfaces

C. N. R. RAO*† and JOHN M. THOMAS*

Department of Physical Chemistry, University of Cambridge, Lensfield Road, Cambridge CB2 1EP, U.K.

Received July 26, 1984 (Revised Manuscript Received December 13, 1984)

Most chemists are familiar with two kinds of intergrowths: *epitaxy*, which involves the oriented overgrowth of one crystalline solid upon another, and *polytypism*, which arises when individual sheets in a layered material are stacked in different sequences. Epitaxy is currently of technological interest since it dictates the laying down of thin, single-crystal films of semiconductors on to a substratum suitable for the production of integrated microelectronic circuits. It also occupies a central role in the phenomena of biomineralization and urinary calculi where an inorganic crystal such as $CaCO_3$ or SiO_2 grows in registry with crystalline slivers of polysaccharide, protein, or purine.[1] Polytypism is less important technologically. Nonetheless, two extreme polytypic forms of ZnSe—one with hexagonal (ABAB), the other with cubic (ABCABC) packing—have[2] significantly different electronic band gaps (2.863 and 2.810 eV) and hence different luminscent and other photophysical properties. When polytypic regions are separated spatially on a nanometer scale in semiconducting materials such as GaAs and CdTe, so-called "*quantum wells*" may form. There are many other types of solid–solid interfaces of interest to the chemist. Although few of these are of immediate commercial relevance, they are all of considerable fundamental significance. Our discussions of such seemingly unrelated phenomena as *chiral turnover* in molecular crystals, of *infinitely adaptive inorganic structures*, of *coincidence boundaries* in zeolites, the origins of *gross nonstoichiometry*, and the occurrence of *modulated structures* all entail an understanding of crystalline intergrowths.

Almost all of the facts we discuss in relation to the phenomenology of intergrowths—in particular their structural characteristics—has been obtained by use of high-resolution electron microscopy (HREM). This technique has unique advantages (described elsewhere[3]) for the direct, real-space study of interfaces. Traditionally an interface within a crystalline solid has been pictured as a structural fault or planar defect. The most familiar is a *twin* plane, where the structures on either side of the plane may be mirror related. Another type of planar fault involves the rotation of one part of a crystal, on a specific plane, with respect to another. There are, in general, a number of lattice points at the interface which are common to the flanking structures that constitute that interface. An example is shown[4] in Figure 1. The presence of both the twin and the coincidence boundary involves an increase in the free energy of the crystal, so that such intergrowths are examples of nonequilibrium defects.[5] Provided their intrinsic energy is not excessively large, such faults, which are often introduced during crystal growth, can be kinetically stabilized and are eliminated only by prolonged annealing. Their occurrence does not give rise to local changes in the stoichiometry of the material within which they occur. New types of structures can be formed[6] by recurrent twinning. For example, a tunnel zeolite with overall hexagonal symmetry is produced by repeated twinning of zeolite Y, which has a cage-type structure with cubic symmetry.[6] In principle, III–V semiconductors crystallizing in diamond-like structures could, by recurrent twinning on the (111) plane, be converted to solids with novel electronic properties.

The same compositional invariance is true of polytypism also, but here other subtleties arise, and these are best appreciated after recalling what is meant in the broadest sense by *stacking* faults. It is well-known[7] that

C. N. R. Rao, a native of Bangalore, India, received his early education in Bangalore and Varanasi. He took his Ph.D. in chemistry from Purdue University and a D.Sc. from the University of Mysore, and he has been honored by a D.Sc. (honoris causa) from Purdue. From 1963 to 1976 he was Professor of Chemistry at the Indian Institute of Technology, Kanpur, from which position he moved to the Indian Institute of Science, Bangalore, first as Head of the Solid State and Structural Chemistry Unit. Since 1984 he has been its Director. During the year 1983–1984, he was Nehru Visiting Professor at the University of Cambridge. He is Vice President of the International Union of Pure and Applied Chemistry and will succeed to the Presidency in September 1985. His main interests are in solid-state chemistry, spectroscopy, molecular structure, and surface science.

John M. Thomas was born in South Wales and took his Bachelor's degree at the University of College at Swansea and completed his Ph.D. at Queen Mary College, of the University of London. For 9 years from 1969 he was Head of the Department of Chemistry at the University College of Wales in Aberystwyth. He then moved to the University of Cambridge as Head of the Department of Physicel Chemistry. He is a Fellow of the Royal Society and of the Indian Academy. He was Baker Lecturer at Cornell University in 1983. He conducts research in solid-state and surface chemistry, dealing with materials such as carbons, organic molecular crystals, clays, and zeolites, and is interested in catalysis and in the chemical consequences of crystalline imperfections.

†Jawaharlal Nehru Visiting Professor, University of Cambridge. Present address: Solid State Structural Chemistry Unit, Indian Institute of Science, Bangalore-560012, India.

(1) See R. J. P. Williams et al. in the special issue of *Philos. Trans. R. Soc. London, Ser. B*, **304**, 409–588 (1984).

(2) A. D. Yoffe, K. Howlett, and P. M. Williams, *Philos. Mag.* **25**, 247 (1971).

(3) J. M. Thomas and D. A. Jefferson, *Endeavour New Ser.*, **2**, 127 (1978); J. M. Thomas, *Ultramicroscopy*, **8**, 13 (1982); C. N. R. Rao, Sir C. V. Raman Lecture, Indian Institute of Science, 1983; J. M. Thomas, "Inorganic Chemistry Towards 21st Century", M. H. Chisholm, Ed., American Chemical Society, Washington, DC, 1983, ACS Symp. Ser. No. 211, p 445; G. R. Millward and J. M. Thomas, Proceedings of a NATO Advanced Study Institute on Surface Properties and Catalysis by Non-Metals and Oxides, J. P. Bonelle, et al., Ed., Dordrecht, 1983, p 19; C. N. R. Rao in "Solid-State Chemistry: A Perspective Report", Indian National Science Academy, Delhi, 1984; C. N. R. Rao, *Chem. Scr.*, **19**, 124 (1982).

(4) O. Terasaki, J. M. Thomas, and S. Ramdas, *J. Chem. Soc., Chem. Commun.*, 216 (1984); see also O. Terasaki, G. R. Millward, and J. M. Thomas, *Proc. R. Soc. London, Ser. A*, **395**, 153 (1984).

(5) J. M. Thomas, *Adv. Catal.*, **19**, 293 (1969); J. M. Thomas, *Chem. Br.*, **6**, 60 (1970); J. M. Thomas, *Endeavour*, **29**, 149 (1970).

(6) J. M. Thomas, M. Audier, and J. Klinowski, *J. Chem. Soc., Chem. Commun.*, 1221 (1981); M. Audier, J. M. Thomas, J. Klinowski, D. A. Jefferson, and L. A. Bursill, *J. Phys. Chem.*, **86**, 581 (1982).

0001-4842/85/0118-0113$01.50/0

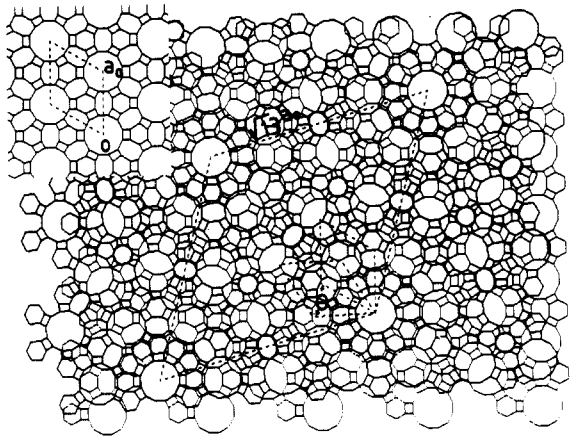

Figure 1. A coincidence boundary on (001) in zeolite L (idealized formula $K_6Na_3Al_9Si_{27}O_{72}\cdot 21H_2O$). The top part of the crystal is rotated[4] by 32.2° with respect to the bottom part, thereby generating the coincidence boundary, the repeat mesh of which bears a $13^{1/2}\cdot 13^{1/2}$ relationship to the parent mesh.

when layers of closely packed units, as in the metals, are stacked in a regular fashion, two simple alternatives are possible: ABABAB... (equivalently designed *hhh*...) and ABCABC... (or *ccc*...) where the symbols *h* and *c* refer respectively to hexagonal and cubic stacking. By introducing a stacking fault, there are infractions to the regular sequencing. Thus a sequence *chcc*, which may be viewed as a regular cubic structure into which one fault has been inserted, gives rise to an intergrowth of cubic and hexagonal regions. Were this stacking fault inserted regularly, the resulting structure could be symbolized ...*chccchccchcc*... and this constitute one particular polytype. Silicon carbide, SiC, is known to exist in over 50 polytpic forms, the unit cell repeat distance in the stacking direction being very large (>1500 Å). Examples of this kind abound. YSeF, ZnS, CdI_2, the transition-metal chalcogenides, certain intermetallics, the chlorites, the spinelloids, and the micas all exhibit such behavior.

If the stacking fault does not extend across the entire plane on which it occurs but is restricted to narrow ribbons, the resulting solid may then be regarded as a parent structure laced with strips of a related daughter structure. Rhombohedral graphite, for example, which has ABC rather than ABAB stacking, as in the hexagonal polymorph, is of this kind: it does not tend to occur as a phase-pure rhombohedral polymorph. The fractional rhombohedral character of a given graphite specimen is increased (up to a maximum of about 30 %) by mechanical deformation by the introduction of dislocations which delineate the strips of stacking faults.[8]

Since stacking faults frequently do extend across entire planes, it is convenient to broaden this idea and thereby interrelate several different structures in terms of regular stacking sequences brought about by the recurrent insertion of a specific replacement vector parallel to the layer planes. We note that the notion of the "fault" now gives way to an intrinsic structural characteristic, a point to which we shall return frequently. In particular, consider the family of zeolites,[9] known as the ABC-6 or chabazite group consisting of offretite, erionite, levyne, and several others in Table I. At first sight, judging from their stoichiometry (even when differences in exchangeable cation and in replaceable water are ignored), these appear to have little in common structurally. Yet on further scrutiny we notice that the tetrahedral (T) sites can be occupied either by Al^{3+} or Si^{4+} at the center pf TO_4 tetrahedra (all corner shared). Furthermore, each one of these zeolites is built of sheets such as that shown in Figure 2. For clarity, the positions of the cations and zeolitic water in these structures have been omitted; the vertices represent T sites and the straight lines joining them bridging oxygens. Viewed in this way, we see that the structures of these seemingly unrelated zeolites do have a familial pattern.[10,11]

The conceptual convenience of picturing structures to be made up of regular sequences of layers is not limited solely to the realm of the qualitative. It is already apparent that we can gain quantitative insights into the structural stability of known or hypothetical sequences of individual component sheets. This emerges from computational approaches[12] to the de-

Table I
Repeat Distances and Stacking Distances of Zeolites[a]

zeolite	formula (zeolitic water omitted)	repeat distance along stacking direction, Å	stacking sequence
cancrinite	$Na_6Al_6Si_6O_{24}$	5.1	AB
sodalite	$Na_6Al_6Si_6O_{24}$	7.7	ABC
offretite	$(Na_{27}Ca_7)_2Al_4Si_{14}O_{36}$	7.6	AAB
losod	$Na_{12}Al_{12}Si_{12}O_{48}$	10.5	ABAC
gmelinite	$(Na_2,Ca)_4Al_8Si_{16}O_{48}$	10.0	AABB
chabazite	$Ca_6Al_{12}Si_{24}O_{72}$	15.1	AABBCC
erionite	$(Na_2,Ca)_{4.5}Al_9Si_{27}O_{72}$	15.1	AABAAC
afghanite	$(Na_2,Ca,K_2)_{12}Al_{24}Si_{24}O_{96}$	21.4	ABABACAC
levyne	$Ca_9Al_{18}Si_{36}O_{108}$	23.0	AABCCABBC

[a] The zeolites named in the left-hand column (idealized) given for the framework and exchangeable cation may be pictured as built-up from the "sheet" shown in Figure 2a with the stacking sequence given in the right-hand column.

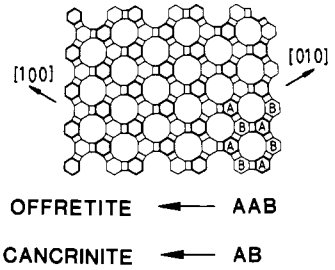

Figure 2. The structures of the zeolites listed in Table I may be regarded as having been derived from various, regular stacking sequences of the single sheet as shown. Thus an AAB sequence yields offretite, AB cancrinite, and so on. Each vertex is a tetrahedral site (T = Si^{4+} or Al^{3+} surrounded by four oxygens).[10]

(7) A. R. Verma and G. C. Trigunayat in "Solid State Chemistry", C. N. R. Rao, Ed., Marcel Dekker, New York, 1978; C. N. R. Rao, *Acc. Chem. Res.*, 17, 83 (1984).
(8) S. Amelinckx, P. Delavignette, and M. Heerschap in "Chemistry and Physics of Carbon", P. Walker, Jr., Ed., Marcel Dekker, New York, 1965, Vol. 1, p 1.
(9) D. W. Breck, "Zeolite Molecular Sieves", Wiley Interscience, New York, 1965; R. M. Barrer, "Zeolites and Clay Minerals", Academic Press, New York, 1978; R. M. Barrer, "Hydrothermal Chemistry of Zeolites", Academic Press, New York, 1982.
(10) G. R. Millward and J. M. Thomas, *J. Chem. Soc., Chem. Commun.*, 77 (1984).
(11) W. M. Meier and D. H. Olson, "Atlas of Zeolite Structure Types", International Zeolite Association, Zurich, 1978.
(12) C. R. A. Catlow, J. M. Thomas, S. C. Parker, and D. A. Jefferson, *Nature (London)*, 295, 658 (1982).

termination of lattice energies using parameterized values for A, ρ, and C in the potential $V(r)$ between two atoms separated by the distance r:

$$V(r) = A \exp(-r/\rho) - Cr^{-6} \quad (1)$$

The pyroxenoid family[13] of silicates ($MSiO_3$, where M can be Mg^{2+}, Ca^{2+}, Fe^{2+}, Mn^{2+}, or mixtures thereof) illustrate this point. Good progress has also been made theoretically[14] in using the Ising model or the anisotropic nearest-neighbor Ising (ANNI)[15] model to interpret polytypism.

To summarize, we note that isolated interfaces within or between solids are regarded as structural faults, but that, in view of both experimental and computational evidence, it is often convenient to regard some structures as made up of regular sequences of "stacking faults".

Nonrecurrent Intergrowths

It is helpful to subdivide the materials that possess internal interfaces of a nonregular nature into those that, on the one hand, remain *compositionally invariant* and into those that, on the other, entail change of composition in crossing the interface. Since almost all crystals, subjected to the right stimulus during growth or therafter,[16] can be induced to undergo twinning, it is not profitable to pursue the various kinds of twinning situations that may arise. There are, however, related phenomena which have striking chemical consequences, especially in the organic solid state.

One such example is the occurrence of *enantiomeric intergrowths* in hexahelicenes. Hexahelicene has a chiral space group $P2_12_12_1$; yet, under certain circumstance, crystals of this compound grown from solution are not chiral, as expected, but essentially racemic, possessing slight enantiomeric excess. This is because the individual crystals are composed of intergrowths in which layers of pure (+) and (−) alternate, thereby generating an essentially racemic "composition". Detailed computations,[17] using atom–atom pairwise evaluation procedures,[18] demonstrate that preferential intergrowths should, and do indeed, occur on (100) planes. They also demonstrate that the extra energy required by the crystal to permit this *chiral turnover* on (100) is a relatively small fraction of the quantity needed for normal growth. In other organic molecular crystals like 1,8-dichloro-9-methylanthracene,[19] evidence[20] from microscopic examination and the nature of the products generated by UV irradiation confirm the occurrence of specific types of internal interfaces.

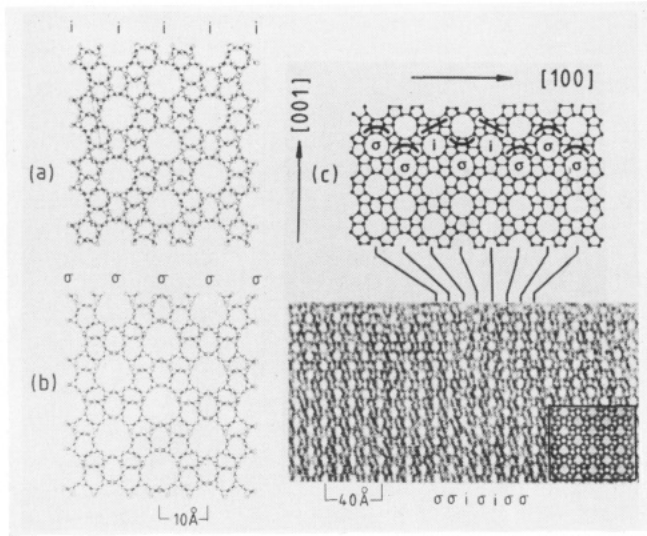

Figure 3. The distinction between (a) ZSM-5 and (b) ZSM-11. An example of a nonrecurrent intergrowth of ZSM-11 in ZSM-5 is shown in (c). Inset [bottom right in high resolution image] shows computer-simulated image.

Molecules situated on either side of such interfaces, which generally function as exciton traps, can photodimerize to yield products that cannot be generated at unfaulted regions of the crystal.

In Figure 1 we saw how zeolite L tends to exhibit internal coincidence boundaries across which the composition remains invariant. A synthetic porotectosilicate, ZSM-5, with much higher Si/Al ratios than naturally occurring zeolites, is a versatile shape-selective catalyst. It tends to form internal interfaces without change of composition.[21-23] To appreciate the subtlety of this process, it is helpful to summarize the structural features[24] of both ZSM-5 and ZSM-11, another shape-selective synthetic zeolite of identical composition: $M_nAl_nSi_{96-n}O_{192}\cdot 162H_2O$, where M is a monovalent cation. Each consists of systems of intersecting channels of diameter ca. 5.5 Å, and this is chiefly responsible for their shape selectivity. Figure 3 summarizes the distinguishing features of ZSM-5 and ZSM-11, which may be regarded as end members of an almost infinite family of regular intergrowths structures e.g., σσiσσi, σσσiσi, iiiσiσi, σσσσii, iiiiσσ, etc., all of which would be polytypes possessing 60-Å repeats[22] in the [100] direction. Some evidence exists[21,22,25] for the occurrence of regular intergrowths; but to date, HREM has uncovered a greater propensity for nonrecurrent growths (Figure 3).

Other synthetic and naturally occurring silicates and aluminosilicates display similar tendencies to form nonrecurrent intergrowths but with more or less bias, depending upon the structural type and sample prehistory, toward the recurrently intergrown state. The sheet silicates mica, chloritoid, and stilphomelane fall into this category,[26] as do the naturally occurring py-

(13) M. Alario Franco, D. A. Jefferson, N. J. Pugh, J. M. Thomas, and A. C. Bishop, *Mater. Res. Bull.*, **15**, 73 (1980); J. M. Thomas, *New Sci.*, 580 (1980).
(14) S. Ramasesha and C. N. R. Rao, *Philos. Mag.*, **34**, 827 (1977); M. K. Uppal, S. Ramasesha, and C. N. R. Rao, *Acta Crystallogr., Sect. A*, **A36**, 356 (1980).
(15) J. Smith and V. Heine, *J. Phys. C*, in press; S. Ramasesha *Pramana*, **23**, 745 (1984); M. E. Fisher and W. Selke, *Phys. Rev. Lett.*, **44**, 1502 (1980).
(16) R. H. Martin and M. Debleckar, *Tetrahedron Lett.*, 3597 (1969); H. Wynberg, *Acc. Chem. Res.*, **4**, 65 (1971).
(17) S. Ramdas, J. M. Thomas, M. E. Jordan, and C. J. Eckhardt, *J. Phys. Chem.* **85**, 2421 (1981).
(18) A. I. Kitaigorodskii, *Chem. Soc. Rev.*, **7**, 133 (1978); S. Ramdas and J. M. Thomas, *Chem. Phys. Solids Their Surf.*, **7**, 31 (1978).
(19) S. Ramdas, J. M. Thomas, and M. J. Goringe, *J. Chem. Soc., Faraday Trans. 2*, **73**, 551 (1977).
(20) J. P. Desvergne, J. M. Thomas, J. O. Williams, and H. Bouas-Laurent, *J. Chem. Soc., Perkin Trans. 2*, 363 (1974).
(21) J. M. Thomas and G. R. Millard, *J. Chem. Soc., Chem. Commun.*, 1380 (1982).
(22) G. R. Millward, S. Ramdas, J. M. Thomas, and M. T. Barlow, *J. Chem. Soc., Faraday Trans. 2*, **79**, 1075 (1983).
(23) J. M. Thomas, G. R. Millward, S. Ramdas, and M. Audier in "Intrazeolite Chemistry" F. G. Dwyer and G. D. Stucky, Ed., American Chemical Society, Washington, DC, 1982, ACS Symp. Ser. No. 218, p 181.
(24) P. B. Weisz, *Pure Appl. Chem.*, **52**, 2091 (1980); G. T. Kokotailo and W. M. Meier, *Chem. Soc. Spec. Publ.*, **33**, 133 (1980).
(25) J. M. Thomas *Int. Conf. Catal., 8th, 1984*, **1**, 31 (1984); *Pure Appl. Chem.*, in press.

roxenoids (encompassing pyroxene, wollastonite, rhodonite, and pyroxmangite). An instructive example is the synthetic mineral[12] $Mn_3MgSi_4O_{12}$, which, after short-duration annealing following crystallization from the melt, exhibits nonrecurrent intergrowths of pyroxenic and pyroxmanganitic structures. After longer annealing times, this material takes up an ordered (pyroxamangite) structure with repeat distances of 17.4 Å.

Intergrowths of amphiboles (double-chain silicates of width 9.5 Å) with analogous structures consisting of triple, quadrupole, or wider strips (typically 13.5 and 18.0 Å) of connected, pyroxene chains[7] have also been intensively studied, chiefly by HREM. These intergrowths are predominantly nonrecurrent; but examples of more ordered structures, entailing repeat distances of ca. 60 Å, are known.[28] In these examples, however, compositional differences arise in traversing the intergrowth; the idealized stoichiometry of a triple-chain feature accommodated within an amphibole such as nephrite jade is $Ca_2(Mg,Fe)_8Si_{12}O_{32}(OH)$ whereas the idealized stoichiometry of the host nephrite (actinolite end member) is $Ca_2(Mg,Fe)_5Si_8O_{22}(OH)_2$.

Solid–solid interfaces involving changes in composition are legion—all examples of epitaxy, whether they consist of catalytically active metals[29] or metal halide[30] supported on graphite, or of semiconducting elements (e.g., Ge) on optically transparent supports (BaF_2),[31] or of wheddelite on uric acid[32] in urine, fall into this category. Of greater relevance in the present context are the isolated planar faults generated as a result of *crystallographic shear* (CS).[33] The key points here are (i) that local coordination is invariant—thus for WO_3, six oxygens remain coordinated to each W, but at the CS fault itself which is introduced on reduction to WO_{3-x} ($x \leq 1.0$) corner sharing of octahedra is replaced by edge sharing—and (ii) that the displacement vector has a component perpendicular to the plane of the fault. If progressively more oxygen is removed from the parent oxide, more CS planes are introduced. These will not initially, take up a strictly recurrent pattern; but, just as with the pyroxenoids, quoted above, prolonged annealing generates recurrent intergrowths, and the resulting repeat distances are governed by the degree of gross nonstoichiometry that prevails. Typically for a composition $WO_{2.8}$ ($x = 0.2$) the separation distance is close to 33 Å. For nonstoichiometric oxide $M_nO_{3n-(m-1)}$ it can be shown that where the CS plane lies upon a (10 m) plane, the equilibrium CS plan spacing is $d_{CS} = n - [(m - {}^1/_2)\, a]/(m^2 + 1)^{1/2}$, where a is the length of the diagonal of the MO_6 octahedron (i.e., about 3.8 Å).

The oxides of Mo and W are able to form so-called Magneli phases[33,34] of general formula M_nO_{3n-1}, M_nO_{3n-2}, M_nO_{3n-3}, etc., with n typically ranging from 12 to 28. The $(3n - 1)$ homologous family results when CS planes

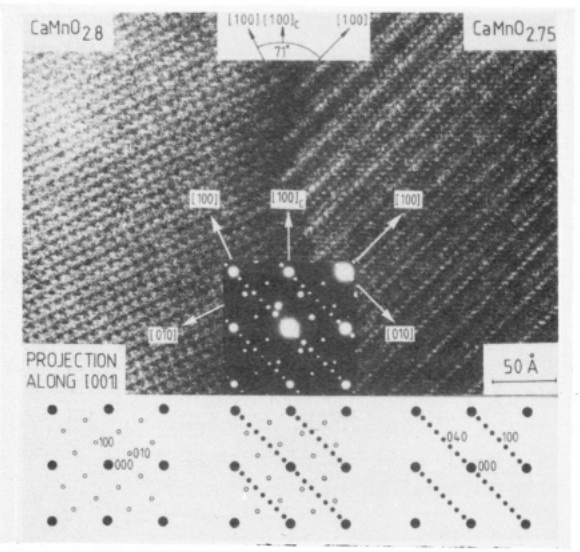

Figure 4. The HREM image and the selected area electron diffraction patterns of a typical example[42] of autoepitaxy, where one substoichiometric perovskite $CaMnO_{2.75}$ grows in coherent contact with its less fully reduced parent, $CaMnO_{2.8}$.

are on {102} of the parent oxide; the $(3n - 2)$ family when the CS planes are on {103}, and so on.

It is instructive to note that when TiO_2 and CrO_2 (both with the rutile structure) are rendered grossly nonstoichiometric, at the CS planes (where 6-fold coordination is preserved and edge sharing of MO_6 octahedra is replaced by face sharing); and at the (CS) itself the local structure is, in effect, a two-dimensional sliver of the corundum structure (local stoichiometry M_2O_3). Recognizing this fact, we now revert to the point made earlier; vis., that a single intergrowth (in this case a CS plane) is best regarded as a structural fault. But ordered, recurrent CS planes are best pictured as an integral feature of the structure of the resulting solid. This concept is encountered again below.

Noncurrent intergrowth is common not only in silicates but also in a variety of other inorganic solids, for example, β''-alumina; the same is true of β- and β''-gallia.[35] In Magneli phases of vanadium (general formula V_nO_{2n-1}), intergrowths of neighboring members has been observed.[36] In perovskite-related oxides of the formula $A_{n+1}B_nO_{3n+1}$, HREM studies have shown the coexistence of lamellae with different n values;[37] thus, the lattice image of $Sr_8Re_2O_7$ shows the presence of lamellae of oxides with n = 2, 4, 5, 7, and 8. Similar random intergrowth of different members of a family is also found[38] in oxides of the general formula $(Bi_2O_2)^{2+}(A_{m-1}B_mO_{3m+1})^{2-}$, first described by Aurivillius.[39] Lattice images of $Ca_xLa_{1-x}FeO_{3-y}$ show disordered intergrowths of $Ca_2Fe_2O_5$ (brownmillerite structure) and $Ca_2LaFe_3O_8$.[40] Interesting nonrecurrent intergrowths have been recently discovered in the $CaMnO_{3-x}$ system.[41] Typical of these intergrowths are $CaMnO_{2.8}$–

(26) J. M. Thomas, D. A. Jefferson, L. G. Mallinson, D. J. Smith, and E. S. Crawford, *Chem. Scr.*, **14**, 167 (1978-79).
(27) J. B. Thompson, *Am. Mineral.*, **63**, 239 (1978).
(28) L. G. Mallinson, D. A. Jefferson, J. M. Thomas, and J. L. Hutchinson, *Philos. Trans. R. Soc.*, London, *Ser. A*, **295**, 537 (1980); D. R. Veblen, P. R. Buseck, and C. W. Burnham, *Science*, **198**, 359 (1977).
(29) E. L. Evans, O. P. Bahl, and J. M. Thomas, *Carbon*, **5**, 587 (1967).
(30) J. M. Thomas, G. R. Millward, R. Schlögl, and H. P. Boehm, *Mater. Res. Bull.*, **15**, 671 (1980).
(31) J. M. Gibson and J. M. Phillips, *Appl. Phys. Lett.*, **43**, 828 (1983).
(32) K. Lonsdale, *Nature* (*London*), **217**, 56 (1968).
(33) A. D. Wadsley, *Rev. Pure Appl. Chem.*, **5**, 165 (1955).
(34) A. Magneli, *Ark. Kemi*, **1**, 513 (1950).
(35) L. Ganapathi, G. N. Subbanna, J. Gopalakrishnan, and C. N. R. Rao, *J. Mater. Sci.*, in press.
(36) Y. Hirotsu, Y. Tsunashima, S. Nagakura, H. Kuwamoto, and H. Sato, *J. Solid State Chem.*, **43**, 33 (1982).
(37) R. J. D. Tilley, *J. Solid State Chem.*, **21**, 293 (1977).
(38) J. L. Hutchison, J. S. Anderson, and C. N. R. Rao, *Proc. R. Soc.*, *London, Ser. A*, **355**, 301 (1977).
(39) B. Aurivillius, *Ark. Kemi.*, **2**, 519 (1950).
(40) M. Alario Franco, J. M. G. Calbet, M. V. Regi, and J. C. Grenier, *J. Solid State Chem.*, **49**, 285 (1983).
(41) A. Reller, D. A. Jefferson, J. M. Thomas, and M. K. Uppal, *J. Phys. Chem.*, **87**, 913 (1983); A. Reller, J. M. Thomas, D. A. Jefferson, and M. K. Uppal, *Proc. R. Soc., London, Ser. A*, **394**, 223 (1984).

Table II
Typical Homologous Series Resulting from Recurrent Intergrowth

$Ba_{2n+p}Me_{2n}Fe_{12(n+p)}O_{22n+19p}$ with Me = Zn, Ni, etc., n = 1–47, and p = 2–12
$BaFe_{12}O_{19}(Me_2Fe_4O_8)_n$ with n = 1–4
$Bi_4A_{2n-1}B_{2n+1}O_{6n+9}$ with A = Ba or Bi, B = Ti, Nb, Cr, etc., and n = 1–3
A_xWO_3 with A = alkali or alkaline earth metal, Bi, etc. ($0.0 < x \leq 0.1$)
$A_xP_4O_8(WO_3)_{2m}$ with m = 4–10
$(Na,Ca)_nNb_nO_{3n+2}$ with n = 4–4.5
$(A_3Nb_6Si_4O_{26})_n(A_3Nb_{8-x}M_xO_{21})$ with A = Ba or Sr, M = Ti, Ni, Zn, etc., and n = 1–15

$CaMnO_3$, $CaMnO_{2.8}$–$CaMnO_{2.75}$ which may, in effect, be regarded as examples of autoepitaxy (Figure 4).

When there is a profusion of nonrecurrent intergrowths between minute regions of distinct structure and stoichiometry, the situation resembles that found in so-called *infinitely adaptive structures*. Such structures occur when, within certain compositional structural extremes, a given compositon has associated with it its own unique structure.[42] Infinitesimal changes in composition are accompanied by changes in the structure (e.g., changes in separation of CS planes or in the dimensional "blocks" formed when CS planes intersect). Good examples of infinitely adaptive structures are the solid solutions Ta_2O_5–WO_3 and $Ba_p(Fe_2S_4)_q$.

Recurrent Intergrowths

Many nonrecurrent intergrowths show a certain degree of order and it is often a matter of definition to stipulate how many repeats of a particular sequence constitute recurrent intergrowth. There are, however, several systems where recurrent intergrowth occurs over fairly large distances[44] and generates homologous series of structures with large unit cells (Table II).

If an intergrowth boundary is pictured as a perturbation, then recurrent intergrowths are sensibly classified, along with other, so-called *modulated structures*. This latter term is used to describe any periodic or partially periodic perturbation of a crystal structure within a repeat distance appreciably greater than the basic unit cell dimension—well-known examples in metallurgy and mineralogy are respectively Au–Mg alloys[43] and antigorite.[26]

An example of recurrent intergrowth is provided by the family of hexagonal barium ferrites, M_pY_q, formed by the components $BaFe_{12}O_{19}$(M) and $Ba_2Me_2Fe_{12}O_{22}$ with Me = Zn, Ni, or Mg (Y).[45,46] We show in Figure 5 an electron micrograph of a typical ferrite. Barium ferrites exhibit a wide range of unit cell dimensions: for example, in MY, c = 26 Å and in M_8Y_{27}, c = 1455 Å. The complexity of these intergrowths is illustrated by $M_{12}Y_{47}$ which has the composition $Ba_{106}Ni_{94}Fe_{1268}$ with 12 M units in the primitive cell. The M_pY_q intergrowths are not formed when Fe^{3+} is replaced by Al^{3+} ions, suggesting the importance of magnetic interactions in stabilizing these large-repeat-distance structures.

(42) J. S. Anderson, *J. Chem. Soc., Dalton Trans.*, 1107 (1973).
(43) O. Terasaki and D. Watanabe, *AIP Conf. Proc.*, **53**, 253 (1979).
(44) C. N. R. Rao and K. J. Rao, "Phase Transitions in Solids", McGraw-Hill, New York, 1978.
(45) J. A. Kohn, D. W. Eckart, and C. F. Cook, *Science*, **172**, 519 (1971).
(46) J. S. Anderson and J. L. Hutchison, *Contemp. Phys.*, **16**, 443 (1975).

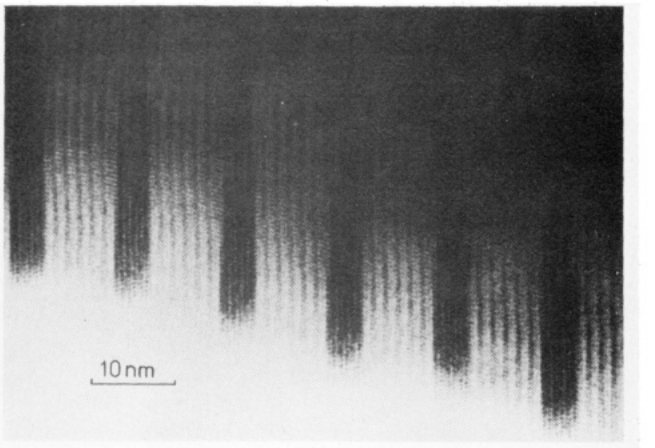

Figure 5. Lattice image of $MYMY_6$ intergrowth in the barium ferrite system.[46]

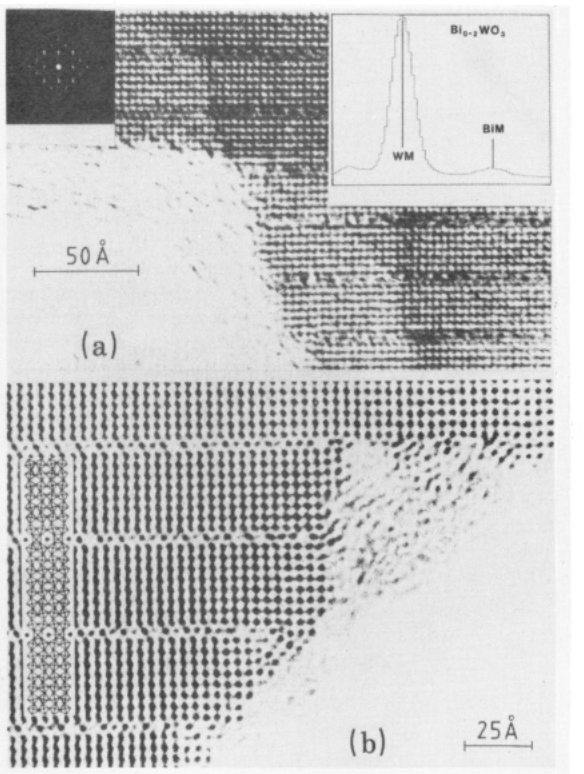

Figure 6. (a) HREM image of a crystal of nominal composition $Bi_{0.2}WO_3$ (obtained with a 200-kV microscope), selected area electron diffraction, and X-ray emission spectrum. The image corresponds to the [001] projection. (b) HREM image (500 kV) of a crystal of nominal composition $Bi_{0.1}WO_3$ again in the [001] projection. The structural model is also shown; dark circles in the model are Bi atoms, which are clearly visible in image.

An interesting class of recurrent intergrowths is formed when slabs of WO_3 cohere with strips of an hexagonal *tungsten* oxide *bronze* (HTB). These intergrowths, referred to as intergrowth tungsten oxide bronzes (ITB), show complex ordered sequences with large periodicities spanning fairly large distances.[47] Figure 6a shows the image of an ITB formed by bismuth.[48] Here WO_3 slabs intergrow with an HTB strip, one tunnel wide; and an electron-induced X-ray emission spectrum (given in the figure) establishes the

(47) L. Kihlborg, *Chem. Scr.*, **14**, 187 (1978).
(48) D. A. Jefferson, M. K. Uppal, D. J. Smith, A. Ramanan, J. Gopalakrishnan, and C. N. R. Rao, *Mater. Res. Bull.*, **19**, 535 (1984); A. Ramanan, J. Gopalakrishnan, M. K. Uppal, D. A. Jefferson, and C. N. R. Rao, *Pr. R. Soc., London, Ser. A*, **395**, 127 (1984).

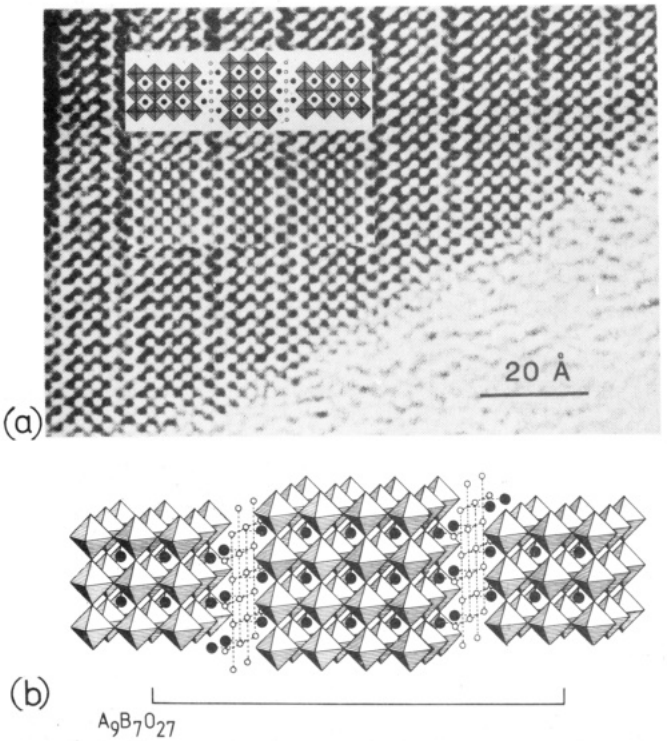

Figure 7. (a) High-resolution image of $Bi_9Ti_6CrO_{27}$ obtained with a 500-kV microscope. The computer-simulated image and structural model are shown as insets and in (b), where the general formula, $A_9B_7O_{27}$, for the $m = 3$, $m = 4$ is given. The dark circles separating the perovskite blocks are the Bi atoms at the interface. The computed image appears below the drawing of the structure in (a).

composition to be $Bi_{0.07}WO_3$, a composition which is also corroborated by X-ray photoelectron spectroscopic analysis. The high-resolution image of the ITB phase in Figure 6b clearly shows tunnels in the HTB strip occupied by bismuth atoms. Other "bronze-like" intergrowths have been reported.[49] The formation of these intergrowth bronzes is likely to be a consequence of the growth conditions and may well represent a case where the impurity-rejection model holds.[50] Long-period intergrowths of barium siliconiobates[51] and $(Na,Ca)_nNb_nO_{3n+2}$ [52] seem to resemble the continuous series of ordered structures or the infinitely adaptive structures described by Anderson.[42]

Recurrent intergrowths formed by the *Aurivillius* group of oxides of the formula $(Bi_2O_2)^{2+}(A_{m-1}B_mO_{3m+1})^{2-}$ have been investigated in Cambridge and Bangalore. This system shows remarkable order even in the absence of magnetic or charge-ordering interactions and forms the homologous series $Bi_4A_{2n-1}B_{2n+1}O_{6n+9}$. Figure 7 shows the high-resolution image of $Bi_9Ti_6CrO_{27}$ formed by the intergrowth of $Bi_4Ti_3O_{12}$ ($m = 3$) and $Bi_5Ti_3CrO_{15}$ ($m = 4$), along with the computer-simulated image and the structural model, to illustrate the ordered arrangement of the $m = 3$ and $m = 4$ lamallae.[53] These systems represent cases where elastic forces alone seem to be responsible for the recurrent intergrowth.

Long-range repulsive interactions arising from elastic forces appear to be of great importance in the formation of recurrent intergrowths. Elastic interactions have indeed been considered to play a crucial role in governing polytypism, epitaxy, and the formation of infinitely adaptive structures. The average elastic energy per unit area per plane resulting from the uniform strain[54] induced by the coherent intergrowth of planes of two units A and B (giving rise to the composition AB) is given by

$$U = \frac{Yd}{4}(\epsilon_A^2 + \epsilon_B^2) \qquad (2)$$

where ϵ_A and ϵ_B are the strains, Y is the elastic modulus, and d is the interplanar spacing. If we assume the planes to be nearly of the same lattice constant, a, U will be proportional to $(\Delta a/a)^2$ since $\epsilon_A = -\epsilon_B$ and $a(\epsilon_A + \epsilon_B) = \Delta a$. While this treatment explains how such a repulsive force could be responsible for long period intergrowths, an operational criterion can be derived by expressing the elastic strain energy in terms of the volume change accompanying the formation on the intergrowths. For the recurrent intergrowths formed by the oxides $(Bi_2O_2)^{2+}(A_{m-1}B_mO_{3m+1})^{2-}$, the volume change, $\Delta V'$, turns out to be

$$\Delta V' = 2V_B'\left(1 - \frac{a^2}{a'^2_B}\right)^2 + mk_mV_p'\left(1 - \frac{a^2}{a'^2_p}\right)^2 + (m+1)K_{m+1}V_p''\left(1 - \frac{a^2}{a''_p}\right)^2 \qquad (3)$$

where V_p' and V_p'' are the volumes of unconstrained perovskite slabs of m and $m + 1$ dimensions, k is related to the bulk modulus, and V_B' represents the volumes of the unconstrained Bi_2O_2 layers. We find that $\Delta V'$ calculated for the various recurrent intergrowths of this family is smaller than the sum of the ΔV values for the component m and $m + 1$ oxides.[55] The $\Delta V'$ for $Ba_2Bi_{12}Ti_{10}O_{39}$ which corresponds to the intergrowth of two $m = 3$ one $m = 4$ layers is close to the sum of ΔV values of the component (two 3 and one 4) oxides. In fact, we have not been able to obtain recurrent intergrowths with 3,3,4 sequences repeating over large distances.

Structure of the Interface

It is important to understand the nature of the elastic strain at the solid–solid interface in recurrent intergrowths. By a careful comparison of experimentally determined and computer-simulated high-resolution images, it has indeed been possible to do so.[56] In the recurrent intergrowth of $Bi_9Ti_6CrO_{27}$ (Figure 7) and related oxides, two layers of Bi_2O_2 constitute the interface. An examination of the micrographs indicates that the two Bi-atom layers at the interface are much closer to each other than expected, and such compression could arise from elastic strain. To investigate the nature of this strain from high-resolution images, we calculated[57] images for the following four models: (i)

(49) M. Hervieu and B. Raveau, *J. Solid State Chem.*, **43**, 299 (1982); A. Benmoussa, D. Groult, F. Studer, and B. Raveau, *J. Solid State Chem.*, **42**, 221 (1982); J. P. Groult, M. Goreaud, Ph. Labbe, and B. Raveau, *J. Solid State Chem.*, **44**, 407 (1982).

(50) J. S. Anderson, J. M. Browne, and J. L. Hutchison, *Nature (London)*, **237**, 5351 (1972); R. J. D. Tilley, *Chem. Phys. Solids Their Surf.*, **8**, 166 (1980).

(51) F. Studer and B. Raveau, *Phys. Status Solids A*, **48**, 301 (1978).

(52) R. Portier, A. Capry, M. Fayard, and J. Galy, *Phys. Status Solidi A*, **30**, 683 (1975).

(53) J. Gopalakrishnan, A. Ramanan, C. N. R. Rao, D. A. Jefferson, and D. J. Smith, *J. Solid State Chem.*, **55**, 101 (1984).

(54) C. Kittel, *J. Solid State Comm.*, **25**, 519 (1978).

(55) K. Kikuchi, *Mater. Res. Bull.*, **14**, 1561 (1979).

(56) D. A. Jefferson, M. K. Uppal, D. J. Smith, and C. N. R. Rao, *Mater. Res. Bull.*, **19**, 1403 (1984).

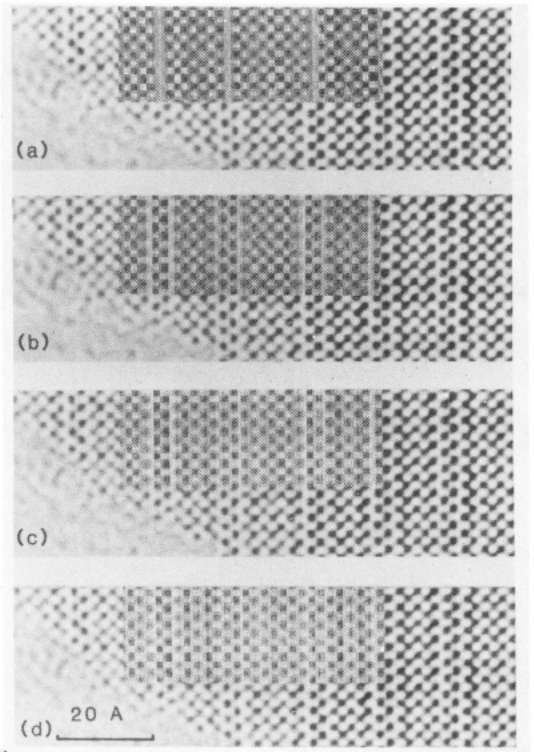

Figure 8. Image simulations of $BaBi_8Ti_7O_{27}$ compared with experimental image. $BaBi_8Ti_7O_{27}$ results from the recurrent intergrowths of $Bi_4Ti_3O_{12}$ ($m = 3$) and $BaBi_4Ti_4O_{15}$ ($m = 4$) of the $(Bi_2O_2)^{2+}$ $(A_{m-1}B_mO_{3m+1})^{2-}$ family. (a) Model i, (b) model ii, (c) model iii, and (d) model iv (see text). Model i predicts a light fringe between the two Bi layers at the interface while the observed image shows a zig-zag arrangement of Bi atoms resulting from a compression.

$m = 3$ and $m = 4$ lamellae intergrown without any movement of atoms from their ideal positions, (ii) Bi atoms at the edges of the lamellae shifted toward each other to the same extent, all other atoms retaining their positions in the idealized solid, (iii) movement of Bi atoms at the edges of the lamellae as in (ii) but coupled with 50 % expansion of the cation lattice within the perovskite lamellae in a direction perpendicular to the lamellae, and (iv) similar to (iii) but with 100 % expansion of the lattice within the lamellae. Comparison of the calculated and observed images of $BaBi_8Ti_6O_{27}$ (Figure 8) clearly shows that model i is inappropriate. There is obviously compression of the Bi layers at the interface as in model ii; but the best match is found with model iii, where there is, in addition, some expansion of the cation rearrangement within the perovskite lamellae. Model iv with full expansion of the lamellae does not show the interface distinctly from the perovskite lamellae. While this is not appropriate for $BaBi_8Ti_7O_{27}$, some of the other intergrowths of this homologous series give high-resolution images which are best interpreted in terms of model iv. This study of the solid–solid interface in intergrowths constitutes a unique example of partial structure refinement using HREM.

Concluding Remarks

A wide diversity of solid-state features and phenomena can be viewed in a unified fashion in terms of the concept of intergrowths that occur either within or between solids. These intergrowths include chiral turnover, polytypism, coincidence boundaries, epitaxy, quantum wells, Magneli phases, gross nonstoichiometry, infinitely adaptive structures, and oxide bronzes. The structure of such solid–solid interfaces can often be directly imaged, at near-atomic resolution, by electron microscopy or deduced by computation with the aid of appropriate atom–atom potentials. There are merits in conceptually subdividing modulated structures, which are those that exhibit repeat distances much in excess of the unit cell dimension, into recurrent intergrowths of component substructures and of regarding polytypes as being derived from regularly arranged stacking faults. The importance of elastic forces in stabilizing intergrowth structures is quantitatively illustrated. Apart from connecting several, hitherto seemingly unrelated, topics in the chemistry of solids, this account emphasizes the value of high-resolution electron microscopy in gaining new insights into the structure and energetics of solids. It is clear that recurrent intergrowths may provide means of tailoring composition and therby of preparing solids possessing desired, finely tuned electronic, optical, dielectric, and magnetic properties. To achieve these ends, however, the nature of the long-range elastic forces responsible for recurrent intergrowths needs to be more fully understood.

(57) D. A. Jefferson, G. R. Millward, and J. M. Thomas, *Acta Crystallogr., Sect. A*, **A32**, 823 (1976); J. M. Thomas, D. A. Jefferson, and G. R. Millward, *J. Microsc. Spectrosc. Electron.*, **7**, 315 (1982).